HHS Public Access

Author manuscript

Sci Transl Med. Author manuscript; available in PMC 2019 September 16.

Published in final edited form as:

Sci Transl Med. 2019 July 31; 11(503): . doi:10.1126/scitranslmed.aaw4993.

The androgen receptor regulates a druggable translational regulon in advanced prostate cancer

Yuzhen Liu[1,#], **Jessie L. Horn**[1,#], **Kalyan Banda**[1,#], **Asha Z. Goodman**[1], **Yiting Lim**[1], **Sujata Jana**[1], **Sonali Arora**[1], **Alexandre A. Germanos**[1], **Lexiaochuan Wen**[1], **William R. Hardin**[1], **Yu C. Yang**[1], **Ilsa M. Coleman**[1], **Robin G. Tharakan**[1], **Elise Y. Cai**[1], **Takuma Uo**[2], **Smitha P.S. Pillai**[3], **Eva Corey**[4], **Colm Morrissey**[4], **Yu Chen**[5], **Brett S. Carver**[6], **Stephen R. Plymate**[2], **Slobodan Beronja**[1], **Peter S. Nelson**[1,7], **Andrew C. Hsieh**[1,7]

[1]Divisions of Human Biology and Clinical Research, Fred Hutchinson Cancer Research Center, Seattle, WA 98109, USA

[2]Department of Medicine, Division of Gerontology and Geriatric Medicine, University of Washington, Seattle, WA 98104, USA

[3]Comparative Medicine, Fred Hutchinson Cancer Research Center, Seattle, WA 98109, USA

[4]Department of Urology, University of Washington, Seattle, WA 98915, USA

[5]Human Oncology & Pathogenesis Program, Memorial Sloan Kettering Cancer Center, NYC, NY 10065, USA

[6]Department of Urology, Memorial Sloan Kettering Cancer Center, NYC, NY 10065, USA

[7]University of Washington Departments of Medicine and Genome Sciences, Seattle, WA 98195, USA

Abstract

The androgen receptor (AR) is a driver of cellular differentiation and prostate cancer development. An extensive body of work has linked these normal and aberrant cellular processes to mRNA transcription, however, the extent to which AR regulates post-transcriptional gene regulation remains unknown. Here, we demonstrate that AR uses the translation machinery to shape the cellular proteome. We show that AR is a negative regulator of protein synthesis and identify an unexpected relationship between AR and the process of translation initiation in vivo. This is

Correspondence should be addressed to: Andrew C. Hsieh, Fred Hutchinson Cancer Research Center, 1100 Fairview Ave N, Seattle, WA 98019, USA, ahsieh@fredhutch.org.

[#]These authors contributed equally.

Author contributions: A.C.H. conceived the project; Y. Liu, J.L.H., K.B., A.Z.G., performed mouse experiments; Y. Liu., J.L.H., A.A.G., L.W., W.R.H, and K.B. conducted molecular and cell biology experiments; Y. Lim conducted the ribosome profiling experiment; S.J. conducted the in vitro proximity ligation assay; R.G.T., Y.C.Y., I.M.C., P.S.N. assisted with the RNASeq experiment; Y.C. conducted the ChIPSeq analysis; E.Y.C. and S.B. assisted with shRNA experiments; B.S.C. assisted with enzalutamide experiments; A.A.G. conducted the 5' UTR studies; S.A. conducted computational analysis; T.U. and S.R.P. assisted with ARE experiments; S.P.S.P. conducted blinded pathology evaluation; E.C. and C.M. provided biospecimens and AR staining in the human studies. A.C.H. wrote the manuscript with input from Y.Liu, J.L.H., K.B., Y.Lim, S.J., and A.A.G.; all authors reviewed and edited the manuscript.

Data and materials availability: Raw RNASeq and ribosome profiling sequencing data can be accessed at Short Read Archive (SRP151005, SRP151006) and NCBI Gene Expression Omnibus (GSE116081, GSE116082). Raw ChIPSeq data from *Pten*$^{L/L}$ prostates were obtained from Gene Expression Omnibus (GSE47119). All other data associated with this study are present in the paper or Supplementary Materials.

mediated through direct transcriptional control of the translation inhibitor 4EBP1. We demonstrate that lowering AR abundance increases the assembly of the eIF4F translation initiation complex, which drives enhanced tumor cell proliferation. Furthermore, we uncover a network of pro-proliferation mRNAs characterized by a guanine-rich *cis*-regulatory element that is particularly sensitive to eIF4F hyperactivity. Using both genetic and pharmacologic methods, we demonstrate that dissociation of the eIF4F complex reverses the proliferation program, resulting in decreased tumor growth and improved survival in preclinical models. Our findings reveal a druggable nexus that functionally links the processes of mRNA transcription and translation initiation in an emerging class of lethal AR-deficient prostate cancer.

One-sentence summary

The androgen receptor (AR) regulates mRNA-specific translation through 4EBP1, which is a druggable vulnerability in AR-deficient prostate cancer.

Introduction

The androgen receptor (AR) is a nuclear hormone receptor that is activated by androgens to promote its function as a transcription factor (1). Specificity is mediated in part through receptor recognition of a palindromic di-hexameric DNA motif called the androgen response element (ARE), which controls gene expression through recruitment of co-activators or co-repressors (2). Although the role of AR in regulating transcription is well established, it is unknown if AR uses additional processes such as translation control to direct protein abundance and cellular phenotypes. This is a particularly timely question, because translation regulation is emerging as a critical determinant of proteome diversity, tissue homeostasis, and disease (3–5).

One disease that has demonstrated a sensitivity to inhibition of AR and mRNA translation is prostate cancer. Ninety percent of early-stage human prostate cancers are dependent on androgens for growth (6). However, prolonged use of androgen deprivation therapy (ADT) renders the majority of hormone-sensitive prostate cancers into lethal castration-resistant prostate cancer (CRPC). The defining characteristic of CRPC is the ability to grow in the androgen-poor environment created by ADT. A large subset of CRPC is characterized by restored AR signaling (7). Subsequent improved AR targeting with therapeutics such as abiraterone and enzalutamide has led to life-extending advances for the treatment of CRPC (8, 9). Nevertheless, the disease remains uniformly fatal. Moreover, these potent inhibitors of AR and androgen metabolism have remodeled the phenotypic landscape of CRPC, resulting in a rise in lethal AR-deficient prostate cancers (10, 11).

In parallel studies, it has been shown that the process of translation initiation is a critical driver of prostate cancer pathogenesis. In particular, the cap-dependent translation initiation factor and oncogene eIF4E is necessary for the genesis and progression of prostate cancer mediated by loss of the tumor suppressor PTEN and may be a driver of drug resistance (12, 13). However, the fundamental question remains: how do AR and the translation initiation complex interplay? This is a critical issue because to date, no inhibitors targeting translation regulators have shown broad efficacy in prostate cancer patients (14–16).

We discovered a cell-autonomous mechanism by which AR inhibits translation initiation through the eIF4E binding protein 1 (4EBP1), which limits eIF4F translation initiation complex formation and the proliferative capacity of cells in vivo. We also show that loss of AR increases eIF4F assembly to drive the translation of a network of pro-proliferation mRNAs that share a conserved and functional guanine-rich motif. Importantly, this network is required for enhanced tumor growth in the setting of low AR. Moreover, we demonstrate that in comparison to AR-intact prostate cancer, AR-low prostate cancer has a greater physiologic dependence on eIF4F hyperactivity, which represents a druggable vulnerability. Pharmacologic and genetic disruption of the eIF4F complex decreases tumor growth and improves survival in vivo. As such, we have identified a link between mRNA transcription and translation that defines a specific treatment-resistant form of prostate cancer and is particularly vulnerable to translation inhibition.

Results

Androgen receptor (AR) regulates protein synthesis through 4EBP1

In order to determine the impact of AR on protein synthesis, we used the *Probasin-cre;Pten*$^{LoxP/LoxP}$ prostate cancer mouse model (herein referred to as *Pten*$^{L/L}$), where tissue-specific loss of *Pten* causes PI3K pathway hyperactivation and prostate cancer formation (17). To modulate AR protein abundance, we castrated the mice, which led to a marked decrease in AR protein in each of the four lobes of the murine prostate (fig. S1, A to C). Moreover, we confirmed the functional impact of castration on AR activity by RNAseq (fig. S1D, and table S1). Using a puromycin incorporation assay, we measured *de novo* protein synthesis in intact (non-castrate) and castrate *Pten*$^{L/L}$ mice. We observed that castrate *Pten*$^{L/L}$ mice exhibit a 30% increase in *de novo* protein synthesis on a per cell basis compared to intact *Pten*$^{L/L}$ tumors (Fig. 1A). These findings indicate that AR negatively regulates protein synthesis, which is de-repressed in the context of low AR protein abundance.

Next, we sought to determine how AR controls protein synthesis dynamics. Translation initiation mediated by the eIF4F complex is a critical driver of protein synthesis and cell proliferation (18, 19). This complex is composed of the oncogene eIF4E, which binds to the 5’-cap of mRNA; the scaffolding molecule eIF4G; and the RNA helicase eIF4A (20–22). In addition, 4EBP1 is an antagonist of translation initiation and prevents eIF4F complex formation by binding to the dorsal and lateral surfaces of eIF4E (Fig. 1B) (23). 4EBP1 is phosphorylated and inhibited by the mechanistic target of rapamycin (mTOR) kinase (24). Translation initiation dynamics are strongly influenced by the stoichiometry of the translation initiation components eIF4E, eIF4G, eIF4A, and 4EBP1 (25). To determine the relationship between AR-low prostate cancer and eIF4F-mediated translation, we conducted quantitative immunofluorescence and western blot analysis of these key translation initiation components in intact and castrate *Pten*$^{L/L}$ mice. We observed no increase in eIF4E, eIF4G, or eIF4A protein abundance (Fig. 1C and fig. S1, E and F). However, 4EBP1 protein was decreased in castrate mice relative to intact mice (Fig. 1C and fig. S1, C and E). Therefore, castration-induced low AR abundance results in a decrease in the translation inhibitor 4EBP1.

To determine if the relationship between AR and 4EBP1 is particular to the *Pten*$^{L/L}$ mouse model or a more general principle of prostate cancer, we used human LNCaP prostate cancer cells in which AR has been stably knocked down by shRNA and counter-selected for using an AR-regulated suicide gene (herein referred to as APIPC cells) (11). Comparing APIPC cells to their isogenic parental AR-positive cells, we found that 4EBP1 protein expression is substantially decreased in the absence of AR (Fig. 1D). Next, we asked whether AR protein expression also correlates with 4EBP1 protein expression in human prostate cancer. We evaluated 29 CRPC LuCaP patient-derived xenograft (PDX) models for AR and 4EBP1 protein abundance. We found a positive correlation (R = 0.376, P = 0.02) between AR and total 4EBP1 protein expression in these specimens, which was independent of genomic *PTEN* status (Fig. 1E and fig. S1, G and H). Together, these findings demonstrate that AR strongly correlates with 4EBP1 in both mice and humans.

AR directs *4ebp1* transcription through an ARE encoded in intron 1

The finding that 4EBP1 protein expression consistently correlates with AR protein in three models of advanced prostate cancer (Fig. 1, C to E) drove us to question how AR regulates 4EBP1 abundance. Because AR is a transcription factor, we asked if it regulates 4EBP1 directly through DNA-based mechanisms or indirectly through translation or protein decay (turnover). To determine whether AR affects 4EBP1 protein synthesis rates, we measured the amount of ribosome-protected *4ebp1* mRNA compared to total *4ebp1* mRNA through in vivo ribosome profiling (fig. S2, A and B) (26, 27). We observed no difference in *4ebp1* mRNA translation efficiency between intact and castrate *Pten*$^{L/L}$ mice (fig. S2C). To investigate whether 4EBP1 protein turnover is sensitive to AR protein expression, we examined the phosphorylation status of 4EBP1 at T37/46 which is associated with its degradation (28). Western blot analysis revealed no increase in phosphorylation at those sites (fig. S1E). In addition, we also measured 4EBP1 degradation rates using cycloheximide in *Pten*$^{L/L}$ primary prostate cancer cells grown with or without dihydrotestosterone (DHT). We observed no difference in 4EBP1 turnover rates between intact and castrate *Pten*$^{L/L}$ cells (fig. S2D).

Next, we considered a transcription-based mechanism. We found that in all three model systems (*Pten*$^{L/L}$ mouse model, APIPC human cell line, and LuCaP PDX models), *4ebp1* decreases at the mRNA level in the setting of low AR (Fig. 1F, fig. S2, E and F), which was not further affected by maximal AR blockade (fig. S2G). Moreover, we observed the same phenomenon in 4 different human prostate cancer cell lines (fig. S3, A and B). As such, we suspected that *4ebp1* is an AR-responsive gene. To determine whether AR regulates *4ebp1* mRNA expression, we reintroduced androgens to *Pten*$^{L/L}$ primary cells derived from castrate mice to restore AR protein expression and activity. This resulted in a complete rescue of *4ebp1* mRNA back to AR-intact levels and a decrease in *de novo* protein synthesis (Fig. 1G, fig. S3, C and D). These findings suggested that AR may directly control the transcription of *4ebp1*. To determine if AR binds the *4ebp1* genomic locus in vivo, we analyzed AR ChIPSeq from *Pten*$^{L/L}$ mice (29). We found that AR binds to the first intron of *4ebp1,* which encodes a putative ARE (fig. S4A). This was also observed in wild-type murine prostate, where knockout of AR also decreased *4ebp1* mRNA, as well as in the LNCaP human prostate cancer cell line (fig. S4, B to D).

To determine the functionality of this element, we cloned the 347 bases encompassing the ChIPSeq peak including the putative ARE into a luciferase reporter construct and found that it was strikingly responsive to androgen stimulation in LNCaP prostate cancer cells (Fig. 1H). Next, we deleted the 15 base pair ARE and found that this blunted the response to androgen stimulation (Fig. 1H and fig. S4E). We also cloned a homologous region of the human *4EBP1* locus into the luciferase reporter construct and found that it too increased luciferase activity in response to androgens (fig. S4F). Together, these findings reveal that *4ebp1* is controlled by AR via an ARE encoded within the first intron in both mice and humans.

4EBP1 protein abundance dictates eIF4E-eIF4G interaction dynamics and proliferation in a cell-autonomous manner in AR-low prostate cancer

Our observations suggest that AR may control translation initiation complex formation in vivo. To test this hypothesis, we optimized proximity ligation assays (PLA) for eIF4E-eIF4G interactions and eIF4E-4EBP1 interactions (Fig. 2A) (30). In tumors from castrate $Pten^{L/L}$ mice, we found that eIF4E-eIF4G interactions increase while eIF4E-4EBP1 interactions decrease compared to those from intact mice (Fig. 2B). This was also confirmed by the cap-binding assay (fig. S5A). Thus, low AR alters the balance between eIF4E-4EBP1 inhibitory complexes and eIF4E-eIF4G initiation complexes, resulting in a net increase in eIF4F translation initiation complex formation and an increase in protein synthesis (Figs. 1A and 2B).

Next, we sought to determine the physiologic consequences of decreasing AR-4EBP1 while increasing eIF4F translation initiation complex formation in $Pten^{L/L}$ mice. We observed that long-term castrated $Pten^{L/L}$ mice exhibit increased tumor growth and cell proliferation, and more aggressive disease (Fig. 2, C and D, fig. S5B). This was independent of phenotypic changes such as neuroendocrine differentiation (fig. S5, C and D), or re-engagement of the AKT or MNK1/2 signaling pathways (as measured by AKT or eIF4E phosphorylation, respectively) that can increase translation initiation (fig. S5, E to G) (31, 32). We next determined whether the relationship between AR and 4EBP1 is intrinsic or extrinsic to prostate cancer epithelial cells. Using low passage primary intact (DHT+) and castrate (DHT-) $Pten^{L/L}$ cells, we found that similar to our key in vivo findings, primary intact $Pten^{L/L}$ cells do not express PTEN or neuroendocrine markers (Fig. 2E, fig. S5H). Moreover, castrate cells expressed very low amounts of AR and 4EBP1 protein and proliferated faster than intact cells (Fig. 2, E and F). These findings demonstrate that a decrease in AR protein can diminish 4EBP1 abundance and increase cell proliferation in a cell autonomous manner. Together, these findings mimic in part an emerging subset of CRPC patients with low AR protein expression and resistance to 2nd generation therapeutics such as enzalutamide (11).

AR and eIF4F-mediated mRNA-specific translation controls a regulon of functional cell proliferation regulators

Given that AR-low prostate cancer increases eIF4F complex formation and *de novo* protein synthesis (Figs. 1A and 2B), we next asked whether this impacts the translation of all mRNAs or a subset of mRNAs. To do so, we conducted ribosome profiling of tumors from both intact and castrate $Pten^{L/L}$ mice to identify differentially translated mRNAs (fig. S2A).

Notably, castration and increased eIF4F complex formation were associated with an increase in the translation efficiency of a subset of 697 mRNAs as opposed to all mRNA species (log_2 fold change ≥ 0.75, P-value < 2.2e-16) (Fig. 3A). This finding raised the important question of what makes these specific mRNAs particularly sensitive to increases in eIF4F activity.

A major determinant of translation initiation rates is the composition of the 5' untranslated region (UTR) of an mRNA (33). We observed that the translationally upregulated mRNAs possess a higher GC content and are more thermodynamically stable compared to 19,009 control 5' UTRs (Fig. 3B). There was no significant difference in 5' UTR length (fig. S6A). Together, these findings suggest that eIF4F sensitive mRNAs may have a *cis*-regulatory element encoded within the 5' UTR. We conducted a motif analysis and discovered a guanine-enriched sequence we named the guanine-rich translational element (GRTE) (Fig. 3C, and table S2). The GRTE was present in 66.8% of upregulated mRNAs and 39.6% of genomic 5' UTR sequences (P = 6.32e-14) and was distinct from the previously described mTOR-sensitive PRTE *cis*-regulatory element (fig. S6, B and C) (27). To determine if GRTE-containing 5' UTRs were indeed responsive to fluctuations in eIF4F activity, we cloned the 5' UTRs of *Klf5* and *Denr*, which have this element, into luciferase reporter constructs, and also generated GRTE deletion mutants (fig. S6D). This was subsequently transduced into PC3-*4EBP1*^{M} prostate cancer cells in which doxycycline can induce the expression of a non-phosphorylatable form of 4EBP1 to inhibit eIF4F complex formation (fig. S6E) (27). We observed that wild-type *Klf5* and *Denr* 5' UTRs displayed a decrease in luciferase activity upon induction of the 4EBP1^{M}. However, the non-insert control vector and the GRTE deletion *Klf5* and *Denr* 5' UTRs were both insensitive to eIF4F complex disruption (Fig. 3D and fig. S6F). Next, we sought to determine the specificity of the GRTE by generating wild-type and mutant luciferase reporters with the *Tcea1* 5' UTR, which has a guanine enriched sequence but was not found to be translationally upregulated by ribosome profiling (data file S1). Interestingly, in this context, mutating the element had no impact on translation (fig. S6G). Together, these findings indicate that the GRTE is a specific 5' UTR *cis*-regulatory element that in part enables the enhanced translation of distinct mRNAs in the context of eIF4F hyperactivity.

We next asked if the translationally upregulated mRNAs identified by ribosome profiling organize into networks that may be responsible for specific phenotypes important for AR independence. Through gene set enrichment analysis, we found that these translationally regulated mRNAs cluster into distinct biological processes including signal transduction, translation, cell communication, transcription regulation, and cell proliferation (Fig. 3E). This was corroborated at a gene-specific level. For example, a number of shared mTOR inhibitor-sensitive target genes were up-regulated in the AR-low setting, including *Pabpc1*, *Rps13*, *Rps15*, *Rpl7a*, and *Rpl14* (27, 34) (fig. S6, B and H). Furthermore, we also identified 23 putative regulators of cell proliferation increased at the level of translation in castrate *Pten*$^{L/L}$ mice (Fig. 3F). Together, these findings demonstrate that low AR and increased eIF4F complex formation may promote cancer progression through the translation of distinct networks of mRNAs.

To confirm that the putative proliferation regulators identified by ribosome profiling are controlled at the post-transcriptional level, we conducted western blot and quantitative PCR (qPCR) analysis on a subset of targets including KLF5, a transcription factor critical for maintaining the proliferative capacity of cells; CACUL1, a cullin domain-containing protein that activates CDK2; and DENR, a translation re-initiation factor important for high-density cell proliferation (35–37). Notably, all three genes have at least one GRTE. As a positive control, we also analyzed the small ribosomal subunit protein rpS15. We found that castrate primary *Pten*$^{L/L}$ organoids exhibited increases in the abundance of KLF5, DENR, CACUL1, and rpS15 proteins (Fig. 3G, fig. S7A). However, at the mRNA level, no increase was observed (fig. S7B). Together these findings indicate that KLF5, DENR, and CACUL1 are regulated at the post-transcriptional level. To determine if these genes are regulated by the eIF4F complex, we conducted a reciprocal experiment using organoids derived from castrate *Pten*$^{L/L}$ mice, which also have a doxycycline-inducible 4EBP1^{M}. In this system, castration and prostate-specific loss of PTEN cause non-neuroendocrine AR-low prostate cancer, and doxycycline drives the prostate-specific expression of an inducible non-phosphorylatable *4ebp1* mutant transgene (herein referred to as *Pten*$^{L/L}$*;4ebp1*^{M}, fig. S7C). Upon induction of the 4EBP1^{M}, which diminishes eIF4F complex assembly, we observed a marked decrease in the amounts of KLF5, DENR, CACUL1, and rpS15 proteins (Fig. 3H, fig. S7D). This did not result from a decrease in mRNA (fig. S7E). Thus, AR coordinates the translation of a distinct subset of mRNAs including a network of pro-proliferation regulators through aberrant eIF4F complex formation. To determine if KLF5, DENR, and CACUL1 are necessary to drive the enhanced growth of AR-low CRPC, we used RNAi to knock down each gene in castrate *Pten*$^{L/L}$ primary prostate cancer cells (fig. S7F). Indeed, gene silencing of *Klf5*, *Denr*, and *Cacul1* resulted in a sustained decrease in EdU incorporation compared to a scramble control (Fig. 3I). Together, these findings demonstrate that AR-low prostate cancer exhibits an increase in protein synthesis through the translation of specific subsets of GRTE-containing mRNAs, including an eIF4F-sensitive pro-proliferation regulon, which drives the enhanced growth of AR-low prostate cancer.

Increased eIF4F complex formation is necessary for AR-low prostate cancer initiation and progression

Our findings raised the question of whether the increase in eIF4F complex formation is necessary for AR-low prostate cancer pathogenesis. To test this, we used the *Pten*$^{L/L}$*;4ebp1*^{M} mouse model (fig. S7C). Using the eIF4E-eIF4G proximity ligation assay, we found that the 4EBP1^{M} decreases eIF4F complex formation by approximately 50% in vivo (fig. S8A). We castrated a cohort of *Pten*$^{L/L}$*;4ebp1*^{M} mice and immediately initiated doxycycline treatment to induce the 4EBP1^{M} (Fig. 4A). Eight weeks after induction, we observed a decrease in tumor volumes and cell proliferation in *Pten*$^{L/L}$*;4ebp1*^{M} mice on doxycycline (Fig. 4, B and C). As such, increased eIF4F complex formation drives AR-low prostate cancer initiation and enhanced cell proliferation in vivo.

Next, we asked if increased eIF4E-eIF4G interactions are necessary for AR-low prostate cancer progression. We first castrated *Pten*$^{L/L}$*;4ebp1*^{M} mice and allowed AR-low tumors to grow over 12 weeks. Then we randomized half the cohort onto doxycycline for 12 weeks (Fig. 4D). In this experiment we observed a 50% decrease in tumor weight, a decrease in

cell proliferation, and a decrease in the formation of carcinoma in the doxycycline-treated group (Fig. 4, E to G, fig. S8, B and C). Therefore, increased eIF4F complex formation also maintains the proliferative potential of established AR-low prostate cancer.

Therapeutic disruption of the eIF4E-eIF4G interaction in AR-low prostate cancer inhibits tumor growth and extends survival

A question that arises from our findings is whether AR-low prostate cancer is more addicted to alterations of the eIF4F complex compared to AR-normal or intact prostate cancer. This has potential clinical implications, because no targeted therapies against translation regulators have been broadly efficacious in prostate cancer patients (14–16). To address this question, we used *Pten*$^{L/L}$;*4ebp1*^{M} primary cells grown with or without DHT. Cells were treated with doxycycline to induce 4EBP1^{M} to near equivalent expression between the intact and castrate settings (fig. S9A). We found that AR-low prostate cancer cell proliferation was more decreased by inhibition of eIF4F compared to AR intact cells (Fig. 5A). This increased sensitivity was also observed in vivo (fig. S9B). As such, AR-low prostate cancer may represent an emerging subtype of treatment-resistant prostate cancer with a heightened addiction to increased eIF4E-eIF4G interactions.

These findings raise the possibility that the eIF4F complex is a therapeutic target in CRPC that is more functionally relevant in the context of low AR. This is further supported by the finding that end-stage CRPC patients and human CRPC PDX models exhibit lower 4EBP1 protein abundance when AR expression is low (Figs. 1E and 5B). In contrast, the positive correlation between AR and 4EBP1 protein expression was not observed in treatment-naïve hormone-sensitive prostate cancer (HSPC) patients (fig. S9C). To delineate the dependence on eIF4F in AR-low prostate cancer, we used 4E1RCat, 4E2RCat, and 4EGI-1, three small molecules that can disrupt the formation of the eIF4E-eIF4G complex (Fig. 5C) (38–40). We found that drug concentrations with negligible effects on cell proliferation in primary intact (DHT+) *Pten*$^{L/L}$ cells induced profound changes in primary castrate (DHT-) *Pten*$^{L/L}$ cells (Fig. 5, D and E and fig. S10A). Next, we asked if human prostate cancer cells exhibit a similar therapeutic profile. We treated parental (AR+) or APIPC (AR-) cells with 4E2RCat or 4EGI-1. Similar to our findings in the murine models, AR-null APIPC cells were more sensitive to eIF4E-eIF4G disruption (Fig. 5, F and G, fig. S10B).

Given these promising in vitro findings, we next tested this hypothesis using in vivo models of advanced AR-low prostate cancer. Specifically, we conducted preclinical trials using 4E1RCat, an eIF4E-eIF4G disruptor with in vivo efficacy (Fig. 6A) (38), on the APIPC xenograft model and the AR-null non-neuroendocrine LuCaP 173.2 PDX model. In both studies we observed a marked decrease in tumor growth and improvement in survival without overt toxicity to mice (Fig. 6, B to E, fig. S11, A and B). To determine if the therapeutic impact was specific to tumors with lower AR protein expression, we also treated AR+ parental APIPC xenograft mice with 4E1RCat. Notably, this isogenic AR+ xenograft model was completely insensitive to the eIF4E-eIF4G disruptor (Fig. 6F, and fig. S11C). Thus, patients with AR-deficient prostate cancer may benefit most from eIF4F complex disruption. Furthermore, eIF4F disruption may also improve the efficacy of maximal AR

blockade therapies such as enzalutamide used in patients with new onset CRPC (fig. S11, D to F).

Discussion

Here we show through mouse genetics and molecular analyses that a relationship between AR signaling and translation initiation is instrumental in maintaining proteins synthesis rates in prostate cancer. In particular, AR represses protein synthesis by controlling the abundance of the translation initiation inhibitor 4EBP1 and eIF4F complex formation (fig. S12). This conclusion is supported by our finding that AR binds to an ARE encoded within the first intron of *4ebp1* and promotes its transcription in both normal and cancerous prostates. Reduction or genetic ablation of AR impairs *4ebp1* expression, leading to a substantial increase in the pro-translation eIF4E-eIF4G complex resulting in greater translation initiation. Using the $Pten^{L/L};4ebp1^{M}$ mouse model, we further demonstrated that eIF4F complex formation is essential to initiate and maintain the proliferative potential of AR-low prostate cancer. These findings are clinically relevant because the advent of potent inhibitors of AR or androgen biosynthesis over the past decade has resulted in a 2.5-fold increase of highly treatment-resistant prostate cancer characterized by AR deficiency (11). Our finding reveals that de-repression of translation initiation represents a bypass tract by which prostate cancers deprived of androgen signaling can maintain their proliferative potential leading to AR independence.

An important concept arising from our work is that AR negatively regulates mRNA translation initiation. This raises the question of why this mechanism exists in the first place. One explanation is that AR promotes normal prostate epithelial cell differentiation and may use 4EBP1 to rapidly inhibit protein synthesis, cell growth, and proliferation to allow for tissue maintenance. This was partially demonstrated in prostate epithelial specific AR knockout mice, which exhibit impaired differentiation and increased cell proliferation that can be rescued through the transgenic expression of a constitutively activated AR (41). It remains to be determined if this phenotype is mediated by 4EBP1. Another possibility is that AR regulates metabolic homeostasis through 4EBP1. Alterations in testosterone and AR impact insulin sensitivity and energy metabolism in response to a high-fat diet (42). In a similar manner, *4ebp1* and *4ebp2* knockout mice phenocopy the metabolic defects seen in AR-null or low mice, and overexpression of 4EBP1 is sufficient to rescue the high fat diet-induced metabolic defects, but only in male mice (43, 44). Our finding that AR directly coordinates *4ebp1* expression provides a potential mechanistic basis for how hormone signaling directs tissue growth and metabolism. However, in the context of advanced enzalutamide- or abiraterone-resistant prostate cancer, low AR unleashes the translation initiation apparatus to drive previously inhibited gene networks that can be hijacked to overcome AR dependencies.

To determine the identity of the translational networks affected by a decrease in AR and an increase in eIF4F complex formation, we conducted ribosome profiling in intact and castrate $Pten^{L/L}$ mice. Despite the 30% increase in overall protein synthesis in vivo, only 697 mRNAs demonstrated an increase in translation efficiency. These findings highlight that increasing eIF4F assembly does not impact every mRNA equally and that specific mRNAs

are more sensitive to changes in translation initiation dynamics. This is in part due to enrichment for the GRTE *cis*-regulatory element encoded within the 5' UTRs of the majority of these upregulated genes. Indeed, the *Klf5* and *Denr* 5' UTRs have the GRTE and are sensitive to decreases in eIF4F complex formation. However, not all guanine-rich sequences are responsive to changes in eIF4F activity. For example, we also show that the *Tcea1* 5' UTR, which also encodes a guanine-rich motif but was not translationally upregulated upon castration, does not exhibit a decrease in translation when the sequence is mutated. Together, these data indicate that the surrounding sequence context of the GRTE may also play a role in eIF4F hypersensitivity. Future studies are required to substantiate this hypothesis.

In addition to this shared sequence motif, we also observed that these upregulated genes identified by ribosome profiling bin into distinct functional classes. We found enrichment for a network of translationally regulated mRNAs involved in cell proliferation. The functional diversity of these genes reveals that eIF4F controls distinct cellular processes such as proliferation through coordinated regulation of transcription (KLF5), CDK function (CACUL1), and translation (DENR). As such, eIF4F-mediated translation enables the networking of multiple molecular modules that converge on shared cellular processes that can be usurped in the context of AR-low prostate cancer. Our findings provide an example of how a DNA *cis*-element coordinates the function of a network of *cis*-regulatory element-containing mRNAs to drive a cellular process.

Lastly, we show that the eIF4E-eIF4G interaction represents a therapeutic vulnerability in AR-low prostate cancer (fig. S12). This has clinical implications because we observe that AR protein expression positively correlates with 4EBP1 abundance in patients with advanced stage prostate cancer, and no therapeutics targeting translation regulators have demonstrated broad clinical efficacy to date (14–16). To demonstrate this dependence, we showed that AR-low prostate cancer is more sensitive to inhibition by the $4ebp1^{M}$ transgene compared to AR-intact prostate cancer both in vitro and in vivo. Furthermore, using small molecule disruptors of the eIF4F complex, we found that both human and murine models of AR-low prostate cancer depend on increased eIF4F complex formation to maintain their high proliferation rate more so than their AR-intact counterparts. Ultimately, targeting the eIF4F complex in human models of AR-low, but not AR-intact prostate cancer results in a decrease in tumor growth and an improvement in survival. Our study was limited to preclinical models given the paucity of translation initiation inhibitors currently in clinical trials for prostate cancer patients with available clinical specimens. However, protein synthesis inhibitors are currently in development and are being tested in Phase 1 and 2 clinical trials (,). Together, this work provides a mechanistic rationale for patient stratification to emerging therapies that target the translation initiation machinery in prostate cancer. Our data suggest that prostate cancer patients with de-repressed translation initiation, particularly in the AR-low setting, represent a growing patient population who should most benefit from emerging eIF4F-targeted therapeutics.

Materials and Methods

Study design

The goal of this study was to delineate the functional relationship between AR signaling and the process of mRNA translation and to define the preclinical relevance of targeting protein synthesis based on AR status. This objective was accomplished by (i) mechanistically dissecting the functional relationship between AR and 4EBP1, (ii) using tissue-based ribosome profiling to identify and validate AR-controlled translationally regulated mRNAs, (iii) validating the relationship between AR and 4EBP1 in prostate cancer across multiple model systems, and (iv) conducting a series of in vitro and in vivo preclinical trials delineating the therapeutic efficacy of targeting eIF4E-eIF4G interactions in AR-low prostate cancer. For all experiments, our sample sizes were determined on the basis of experience and published literature, which historically showed that these in vivo models are highly penetrant and universally develop tumors. We used the maximum number of mice available for a given experiment based on the following criteria: the number of GEMMs available for each age group and post-castration cohort, and tumor availability after implantation of human tissue specimens and cell lines. For all studies, mice were randomly assigned to each treatment group. All pathology analyses were conducted by a blinded veterinarian pathologist. The numbers of replicates are specified within each figure legend.

Mice

PB-cre mice were obtained from the Mouse Models of Human Cancer Consortium. *Pten*$^{L/L}$ and *Rosa-LSL-rtTA* mice were obtained from the Jackson Laboratory. *TetO-4ebp1*^{M} mice were generated as previously described (12). All mice were maintained in the C57BL/6 background under specific-pathogen-free conditions, and experiments conformed to the guidelines as approved by the Institutional Animal Care and Use Committee of Fred Hutchinson Cancer Research Center (FHCRC).

Surgical castration

Surgical castrations were performed with 4- to 6-month-old mice under isoflurane anesthesia. Postoperatively, mice were monitored daily for 5 days. To test CRPC initiation, doxycycline (Sigma) was administered in the drinking water at 2 g/liter immediately after castration, and euthanasia was performed 8 weeks after castration. To test CRPC progression, 12 weeks after castration, doxycycline was administered for 12 weeks, and euthanasia was performed 24 weeks after castration.

LuCaP, localized treatment-naïve HSPC, and metastatic CRPC tissue microarrays

The tissue microarrays were obtained from the University of Washington (UW) Genitourinary Cancer Research Laboratory. All patients were consented and samples were obtained under the UW Institutional Review Board approved protocol 2341.

In vivo puromycinylation assay

Mice were injected intraperitoneally with 200 μl of 2.5 mM puromycin (Fisher Scientific) and euthanized after 1 hour. Ventral prostates were formalin-fixed, paraffin-embedded.

Conventional immunofluorescence against puromycin (Millipore) was performed as described in Supplementary Materials with antigen retrieval at 95°C for 30 min and additional incubation with M.O.M. Blocking Reagent (Vector) for 1 hour at room temperature.

AR+ parental, AR- APIPC, and LuCaP 173.2 PDX 4E1RCat preclinical trials

1×10^6 AR+ parental and AR- APIPC cells were resuspended 1:1 in Matrigel (Corning): RPMI-1640 (Gibco) and subcutaneously injected into the flanks of intact or castrate NOD-scid IL2Rgamma^{null} mice respectively. $1\times1\times1$ mm^3 of LuCaP 173.2 tumor chunks were implanted into the flank of castrate mice. Tumor volume was calculated using the formula $(L(W^2))/2$, where L is the length of the tumor and W the width. When tumors reached 100 mm^3, animals were randomized to receive intraperitoneal injections of 15 mg/kg 4E1RCat (Selleckchem) or vehicle (5.2% PEG400 and 5.2% TWEEN80 in ddH_2O), Monday-Friday.

Statistical analyses

Statistical analyses were performed using GraphPad Prism and the R Stats package, and additional descriptions are provided in the figure legends. For the RNAseq and ribosome profiling analysis, R/Bioconductor packages DESeq2, edgeR, and Xtail were used for statistical analysis. An FDR of <0.1 was considered significant. Experimental raw values were depicted when possible or normalized to internal controls from at least two independent biological replicates, with all data represented as mean +/− SEM unless otherwise specified. When comparing data from two different groups, for example, comparisons between intact and castrate settings or a drug treatment with only two arms, the Student's two-tailed t-test was used to determine significance which was set at a P value <0.05. When we compared more than two groups, such as in the multi-drug treatment study, we used ANOVA with a Tukey's range test for multiple comparisons. The Spearman's correlation coefficient and corresponding P value were used to measure the extent of correlation between AR and 4EBP1 in 29 LuCaP PDX models. The Pearson's χ^2-test was used for the correlation analysis of the GRTE. The Kaplan-Meier method with the log-rank test was used for the xenograft and PDX survival analysis. Original tumor measurements are provided in data file S2.

Supplementary Material

Refer to Web version on PubMed Central for supplementary material.

Acknowledgements

We are grateful to the patients who participated in this study and their families. We thank members of the A.C.H. laboratory for helpful advice. We thank Jennifer M. Shen for editing the manuscript. We thank Adam Geballe, Arvind Subramaniam, Cyrus Ghajar, and Cristian Bellodi for critical discussion of the paper. We thank Li Xin for providing ChIPSeq and RNASeq data from wild-type murine prostate luminal epithelial cells. We thank Sita Kugel for providing Riptag2 neuroendocrine cells.

Funding: This work was supported by NIH awards 1R37CA230617, the Pacific Northwest Prostate Cancer SPORE (P50CA097186), P01CA163227, CA182503–01A1, the CDMRP, W81XWH-17–1-0415, and the Shared Resources of FHCRC/UW Cancer Consortium (P30 CA015704). A.C.H. is a V Foundation Scholar and is funded by a NextGen Grant for Transformative Cancer Research from the American Association for Cancer Research (AACR) and a Burroughs Wellcome Fund Career Award for Medical Scientists. K.B. is a recipient of an American Society

of Clinical Oncology Endowed Young Investigator Award in memory of Sally Gordon, a National Cancer Institute training grant (T32CA009515), and a Pilot and Feasibility Studies Program grant funded by the Cooperative Center for Excellence in Hematology (U54 DK106829). Y. Lim received funding through a Department of Defense Prostate Cancer Research Program Postdoctoral Training Award (PC150946) and the AACR. A.C.H., Y.C., and B.S.C. are funded by a Movember-Prostate Cancer Foundation Challenge Award.

Competing interests: A.C.H. receives research funding from eFFECTOR Inc. P.S.N. has consulted for Janssen and Astellas Pharm Inc. All other authors declare no competing interests.

References and notes

1. Dehm SM, Tindall DJ, Androgen receptor structural and functional elements: role and regulation in prostate cancer. Mol Endocrinol 21, 2855–2863 (2007). [PubMed: 17636035]
2. Hsieh AC, Small EJ, Ryan CJ, Androgen-response elements in hormone-refractory prostate cancer: implications for treatment development. Lancet Oncol 8, 933–939 (2007). [PubMed: 17913662]
3. Sendoel A, Dunn JG, Rodriguez EH, Naik S, Gomez NC, Hurwitz B, Levorse J, Dill BD, Schramek D, Molina H, Weissman JS, Fuchs E, Translation from unconventional 5' start sites drives tumour initiation. Nature 541, 494–499 (2017). [PubMed: 28077873]
4. Schwanhausser B, Busse D, Li N, Dittmar G, Schuchhardt J, Wolf J, Chen W, Selbach M, Global quantification of mammalian gene expression control. Nature 473, 337–342 (2011). [PubMed: 21593866]
5. Signer RA, Magee JA, Salic A, Morrison SJ, Haematopoietic stem cells require a highly regulated protein synthesis rate. Nature 509, 49–54 (2014). [PubMed: 24670665]
6. Leuprolide Study G, Leuprolide versus diethylstilbestrol for metastatic prostate cancer. The New England Journal of Medicine 311, 1281–1286 (1984). [PubMed: 6436700]
7. Watson PA, Arora VK, Sawyers CL, Emerging mechanisms of resistance to androgen receptor inhibitors in prostate cancer. Nature Reviews Cancer 15, 701–711 (2015). [PubMed: 26563462]
8. Tran C, Ouk S, Clegg NJ, Chen Y, Watson PA, Arora V, Wongvipat J, Smith-Jones PM, Yoo D, Kwon A, Wasielewska T, Welsbie D, Chen CD, Higano CS, Beer TM, Hung DT, Scher HI, Jung ME, Sawyers C, Development of a second-generation antiandrogen for treatment of advanced prostate cancer. Science (New York, N.Y 324, 787–790 (2009).
9. de Bono JS, Logothetis CJ, Molina A, Fizazi K, North S, Chu L, Chi KN, Jones RJ, Goodman OB Jr., Saad F, Staffurth JN, Mainwaring P, Harland S, Flaig TW, Hutson TE, Cheng T, Patterson H, Hainsworth JD, Ryan CJ, Sternberg CN, Ellard SL, Flechon A, Saleh M, Scholz M, Efstathiou E, Zivi A, Bianchini D, Loriot Y, Chieffo N, Kheoh T, Haqq CM, Scher HI, Abiraterone and increased survival in metastatic prostate cancer. The New England Journal of Medicine 364, 1995–2005 (2011). [PubMed: 21612468]
10. Beltran H, Prandi D, Mosquera JM, Benelli M, Puca L, Cyrta J, Marotz C, Giannopoulou E, Chakravarthi BV, Varambally S, Tomlins SA, Nanus DM, Tagawa ST, Van Allen EM, Elemento O, Sboner A, Garraway LA, Rubin MA, Demichelis F, Divergent clonal evolution of castration-resistant neuroendocrine prostate cancer. Nature Medicine 22, 298–305 (2016).
11. Bluemn EG, Coleman IM, Lucas JM, Coleman RT, Hernandez-Lopez S, Tharakan R, Bianchi-Frias D, Dumpit RF, Kaipainen A, Corella AN, Yang YC, Nyquist MD, Mostaghel E, Hsieh AC, Zhang X, Corey E, Brown LG, Nguyen HM, Pienta K, Ittmann M, Schweizer M, True LD, Wise D, Rennie PS, Vessella RL, Morrissey C, Nelson PS, Androgen Receptor Pathway-Independent Prostate Cancer Is Sustained through FGF Signaling. Cancer Cell 32, 474–489 e476 (2017). [PubMed: 29017058]
12. Hsieh AC, Nguyen HG, Wen L, Edlind MP, Carroll PR, Kim W, Ruggero D, Cell type-specific abundance of 4EBP1 primes prostate cancer sensitivity or resistance to PI3K pathway inhibitors. Science Signaling 8, ra116 (2015). [PubMed: 26577921]
13. Furic L, Rong L, Larsson O, Koumakpayi IH, Yoshida K, Brueschke A, Petroulakis E, Robichaud N, Pollak M, Gaboury LA, Pandolfi PP, Saad F, Sonenberg N, eIF4E phosphorylation promotes tumorigenesis and is associated with prostate cancer progression. Proceedings of the National Academy of Sciences of the United States of America 107, 14134–14139 (2010). [PubMed: 20679199]

14. Wei XX, Hsieh AC, Kim W, Friedlander T, Lin AM, Louttit M, Ryan CJ, A Phase I Study of Abiraterone Acetate Combined with BEZ235, a Dual PI3K/mTOR Inhibitor, in Metastatic Castration Resistant Prostate Cancer. The Oncologist 22, 503–e43 (2017). [PubMed: 28314838]
15. Graham L, Banda K, Torres A, Carver BS, Chen Y, Pisano K, Shelkey G, Curley T, Scher HI, Lotan TL, Hsieh AC, Rathkopf DE, A phase II study of the dual mTOR inhibitor MLN0128 in patients with metastatic castration resistant prostate cancer. Invest New Drugs 36, 1204–1216 (2018).
16. Armstrong AJ, Netto GJ, Rudek MA, Halabi S, Wood DP, Creel PA, Mundy K, Davis SL, Wang T, Albadine R, Schultz L, Partin AW, Jimeno A, Fedor H, Febbo PG, George DJ, Gurganus R, De Marzo AM, Carducci MA, A pharmacodynamic study of rapamycin in men with intermediate- to high-risk localized prostate cancer. Clin Cancer Res 16, 3057–3066 (2010). [PubMed: 20501622]
17. Wang S, Gao J, Lei Q, Rozengurt N, Pritchard C, Jiao J, Thomas GV, Li G, Roy-Burman P, Nelson PS, Liu X, Wu H, Prostate-specific deletion of the murine Pten tumor suppressor gene leads to metastatic prostate cancer. Cancer Cell 4, 209–221 (2003). [PubMed: 14522255]
18. Dowling RJ, Topisirovic I, Alain T, Bidinosti M, Fonseca BD, Petroulakis E, Wang X, Larsson O, Selvaraj A, Liu Y, Kozma SC, Thomas G, Sonenberg N, mTORC1-mediated cell proliferation, but not cell growth, controlled by the 4E-BPs. Science (New York, N.Y 328, 1172–1176 (2010).
19. Lawrence JC Jr., Abraham RT, PHAS/4E-BPs as regulators of mRNA translation and cell proliferation. Trends Biochem Sci 22, 345–349 (1997). [PubMed: 9301335]
20. Lazaris-Karatzas A, Montine KS, Sonenberg N, Malignant transformation by a eukaryotic initiation factor subunit that binds to mRNA 5' cap. Nature 345, 544–547 (1990). [PubMed: 2348862]
21. Haghighat A, Sonenberg N, eIF4G dramatically enhances the binding of eIF4E to the mRNA 5'-cap structure. The Journal of biological chemistry 272, 21677–21680 (1997). [PubMed: 9268293]
22. Rogers GW Jr., Richter NJ, Merrick WC, Biochemical and kinetic characterization of the RNA helicase activity of eukaryotic initiation factor 4A. The Journal of Biological Chemistry 274, 12236–12244 (1999). [PubMed: 10212190]
23. Pause A, Belsham GJ, Gingras AC, Donze O, Lin TA, Lawrence JC Jr., Sonenberg N, Insulin-dependent stimulation of protein synthesis by phosphorylation of a regulator of 5'-cap function. Nature 371, 762–767 (1994). [PubMed: 7935836]
24. Gingras AC, Gygi SP, Raught B, Polakiewicz RD, Abraham RT, Hoekstra MF, Aebersold R, Sonenberg N, Regulation of 4E-BP1 phosphorylation: a novel two-step mechanism. Genes & Development 13, 1422–1437 (1999). [PubMed: 10364159]
25. Hsieh AC, Ruggero D, Targeting eukaryotic translation initiation factor 4E (eIF4E) in cancer. Clin Cancer Res 16, 4914–4920 (2010). [PubMed: 20702611]
26. Ingolia NT, Ghaemmaghami S, Newman JR, Weissman JS, Genome-wide analysis in vivo of translation with nucleotide resolution using ribosome profiling. Science (New York, N.Y 324, 218–223 (2009).
27. Hsieh AC, Liu Y, Edlind MP, Ingolia NT, Janes MR, Sher A, Shi EY, Stumpf CR, Christensen C, Bonham MJ, Wang S, Ren P, Martin M, Jessen K, Feldman ME, Weissman JS, Shokat KM, Rommel C, Ruggero D, The translational landscape of mTOR signalling steers cancer initiation and metastasis. Nature 485, 55–61 (2012). [PubMed: 22367541]
28. Yanagiya A, Suyama E, Adachi H, Svitkin YV, Aza-Blanc P, Imataka H, Mikami S, Martineau Y, Ronai ZA, Sonenberg N, Translational homeostasis via the mRNA cap-binding protein, eIF4E. Mol Cell 46, 847–858 (2012). [PubMed: 22578813]
29. Chen Y, Chi P, Rockowitz S, Iaquinta PJ, Shamu T, Shukla S, Gao D, Sirota I, Carver BS, Wongvipat J, Scher HI, Zheng D, Sawyers CL, ETS factors reprogram the androgen receptor cistrome and prime prostate tumorigenesis in response to PTEN loss. Nature Medicine 19, 1023–1029 (2013).
30. Boussemart L, Malka-Mahieu H, Girault I, Allard D, Hemmingsson O, Tomasic G, Thomas M, Basmadjian C, Ribeiro N, Thuaud F, Mateus C, Routier E, Kamsu-Kom N, Agoussi S, Eggermont AM, Desaubry L, Robert C, Vagner S, eIF4F is a nexus of resistance to anti-BRAF and anti-MEK cancer therapies. Nature 513, 105–9 (2014). [PubMed: 25079330]

31. Hsieh AC, Costa M, Zollo O, Davis C, Feldman M, Testa JR, Meyuhas O, Shokat K, Ruggero D, Genetic Dissection of the Oncogenic mTOR Pathway Reveals Druggable Addiction to Translational Control via 4EBP-eIF4E. Cancer Cell 17, 249–261 (2010). [PubMed: 20227039]
32. Bianchini A, Loiarro M, Bielli P, Busa R, Paronetto MP, Loreni F, Geremia R, Sette C, Phosphorylation of eIF4E by MNKs supports protein synthesis, cell cycle progression and proliferation in prostate cancer cells. Carcinogenesis 29, 2279–2288 (2008). [PubMed: 18809972]
33. Schuster SL, Hsieh AC, The Untranslated Regions of mRNAs in Cancer. Trends Cancer 5, 245–262 (2019). [PubMed: 30961831]
34. Thoreen CC, Chantranupong L, Keys HR, Wang T, Gray NS, Sabatini DM, A unifying model for mTORC1-mediated regulation of mRNA translation. Nature 485, 109–113 (2012). [PubMed: 22552098]
35. Jia L, Zhou Z, Liang H, Wu J, Shi P, Li F, Wang Z, Wang C, Chen W, Zhang H, Wang Y, Liu R, Feng J, Chen C, KLF5 promotes breast cancer proliferation, migration and invasion in part by upregulating the transcription of TNFAIP2. Oncogene 35, 2040–2051 (2016). [PubMed: 26189798]
36. Schleich S, Strassburger K, Janiesch PC, Koledachkina T, Miller KK, Haneke K, Cheng YS, Kuechler K, Stoecklin G, Duncan KE, Teleman AA, DENR-MCT-1 promotes translation re-initiation downstream of uORFs to control tissue growth. Nature 512, 208–212 (2014). [PubMed: 25043021]
37. Chen TJ, Gao F, Yang T, Thakur A, Ren H, Li Y, Zhang S, Wang T, Chen MW, CDK-associated Cullin 1 promotes cell proliferation with activation of ERK1/2 in human lung cancer A549 cells. Biochem Biophys Res Commun 437, 108–113 (2013). [PubMed: 23806693]
38. Cencic R, Hall DR, Robert F, Du Y, Min J, Li L, Qui M, Lewis I, Kurtkaya S, Dingledine R, Fu H, Kozakov D, Vajda S, Pelletier J, Reversing chemoresistance by small molecule inhibition of the translation initiation complex eIF4F. Proceedings of the National Academy of Sciences of the United States of America 108, 1046–1051 (2011). [PubMed: 21191102]
39. Cencic R, Desforges M, Hall DR, Kozakov D, Du Y, Min J, Dingledine R, Fu H, Vajda S, Talbot PJ, Pelletier J, Blocking eIF4E-eIF4G interaction as a strategy to impair coronavirus replication. J Virol 85, 6381–6389 (2011). [PubMed: 21507972]
40. Moerke NJ, Aktas H, Chen H, Cantel S, Reibarkh MY, Fahmy A, Gross JD, Degterev A, Yuan J, Chorev M, Halperin JA, Wagner G, Small-molecule inhibition of the interaction between the translation initiation factors eIF4E and eIF4G. Cell 128, 257–267 (2007). [PubMed: 17254965]
41. Wu CT, Altuwaijri S, Ricke WA, Huang SP, Yeh S, Zhang C, Niu Y, Tsai MY, Chang C, Increased prostate cell proliferation and loss of cell differentiation in mice lacking prostate epithelial androgen receptor. Proceedings of the National Academy of Sciences of the United States of America 104, 12679–12684 (2007). [PubMed: 17652515]
42. Dubois V, Laurent MR, Jardi F, Antonio L, Lemaire K, Goyvaerts L, Deldicque L, Carmeliet G, Decallonne B, Vanderschueren D, Claessens F, Androgen Deficiency Exacerbates High-Fat Diet-Induced Metabolic Alterations in Male Mice. Endocrinology 157, 648–665 (2016). [PubMed: 26562264]
43. Le Bacquer O, Petroulakis E, Paglialunga S, Poulin F, Richard D, Cianflone K, Sonenberg N, Elevated sensitivity to diet-induced obesity and insulin resistance in mice lacking 4E-BP1 and 4E-BP2. The Journal of Clinical Investigation 117, 387–396 (2007). [PubMed: 17273556]
44. Tsai SY, Rodriguez AA, Dastidar SG, Del Greco E, Carr KL, Sitzmann JM, Academia EC, Viray CM, Martinez LL, Kaplowitz BS, Ashe TD, La Spada AR, Kennedy BK, Increased 4E-BP1 Expression Protects against Diet-Induced Obesity and Insulin Resistance in Male Mice. Cell Reports 16, 1903–1914 (2016). [PubMed: 27498874]
45. Bailey TL, Elkan C, Fitting a mixture model by expectation maximization to discover motifs in biopolymers. Proceedings / … International Conference on Intelligent Systems for Molecular Biology; ISMB. International Conference on Intelligent Systems for Molecular Biology 2, 28–36 (1994).
46. Grant CE, Bailey TL, Noble WS, FIMO: scanning for occurrences of a given motif. Bioinformatics 27, 1017–1018.

47. Xiao Z, Zou Q, Liu Y, Yang X, Genome-wide assessment of differential translations with ribosome profiling data. Nature Communications 7, 11194 (2016).

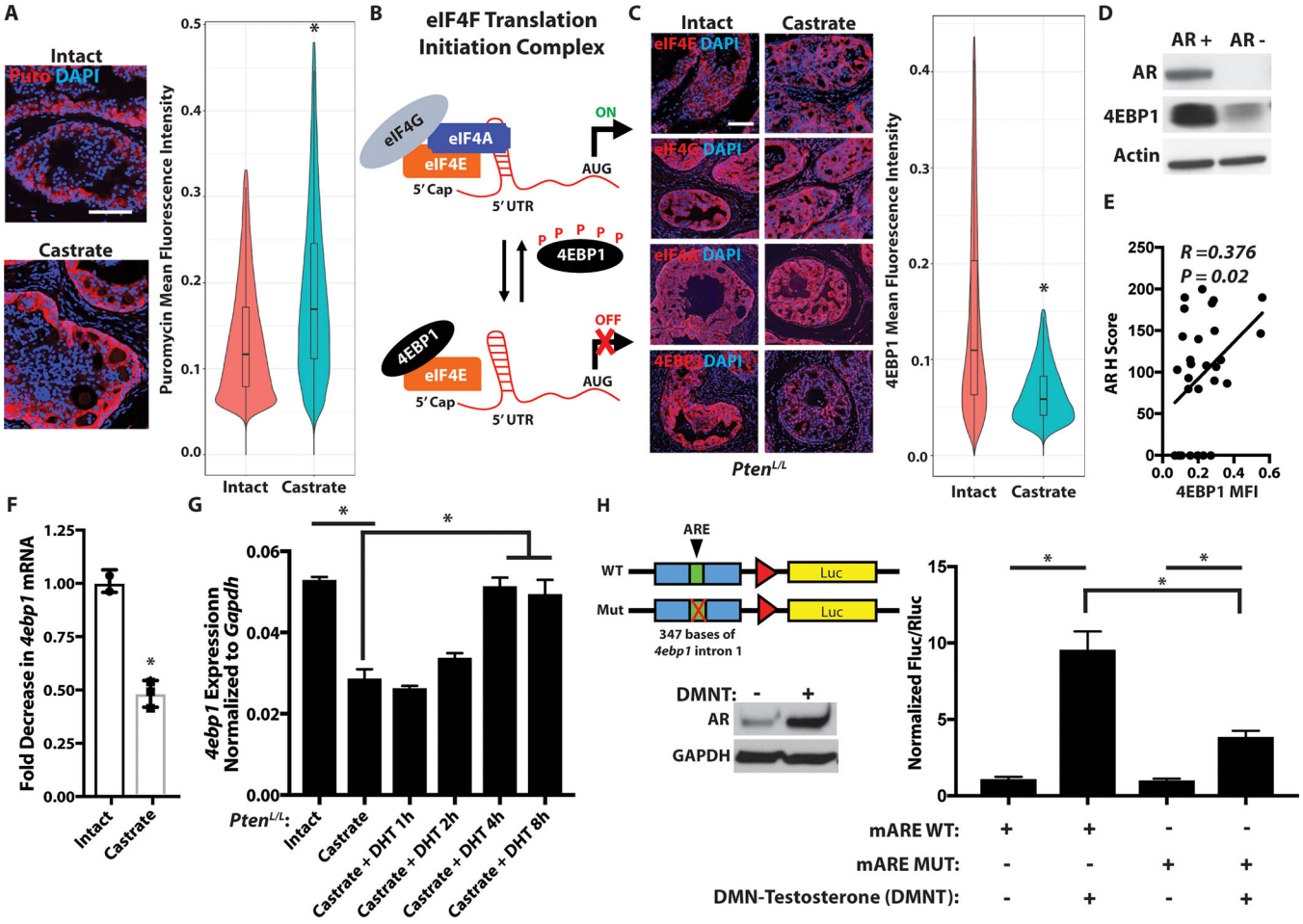

Figure 1. AR controls translation initiation via a *cis*-element encoded within the *4ebp1* locus.

(A) Representative puromycin immunofluorescence for *de novo* protein synthesis in vivo in intact and 8-week castrate *Pten*$^{L/L}$ ventral prostates (left panel). Violin plot of per cell quantitation of puromycin mean fluorescence intensity. The height of the plot represents the range of new protein synthesis observed, and the width represents the number of cells at each fluorescence intensity [right panel, intact n = 3 (46,711 cells quantified), castrate n = 4 (73,237 cells quantified), *P < 2.2e-16, t-test].

(B) Simplified schematic of the eIF4F translation initiation complex composed of eIF4E, eIF4G, and eIF4A with the inhibitor of the complex, 4EBP1 (P = phosphorylation, AUG = start codon).

(C) Representative immunofluorescence for eIF4E, eIF4G, eIF4A, and 4EBP1 in intact and 8-week castrate *Pten*$^{L/L}$ ventral prostates (left panel). Violin plot of per cell quantitation of 4EBP1 mean fluorescence intensity [right panel, intact n = 6 (148,974 cells quantified), castrate n = 5 (111,046 cells quantified), *P < 2.2e-16, t-test].

(D) Representative western blot for AR, 4EBP1, and actin in human AR+ parental and AR- APIPC (AR Program Independent Prostate Cancer) cells.

(E) Correlation plot of 29 human non-neuroendocrine CRPC LuCaP prostate cancer PDX models comparing AR protein content (y-axis, AR H Score) and 4EBP1 protein expression

[x-axis, 4EBP1 mean fluorescence intensity (MFI)] (R = 0.376, P = 0.02, Spearman's correlation).

(F) *4ebp1* mRNA expression by RNASeq in intact and 8-week castrate $Pten^{L/L}$ ventral prostates (intact n = 2, castrate n = 3, *P = 0.002, t-test).

(G) *4ebp1* mRNA expression by qPCR in primary intact (DHT+) and castrate (DHT-) $Pten^{L/L}$ prostate cancer cells. 1 nM DHT was added back to castrate cells over the indicated time points (3 biological replicates, *P < 0.05, t-test).

(H) Schematic of the wild-type (WT) and mutant *4ebp1* intron reporter constructs cloned into the pGL4.28 vector (red triangle = minimal promoter region, luc = firefly luciferase). Representative western blot of AR upon addition of testosterone analog DMNT in LNCaP cells (left panel). Luciferase assay of the putative wild-type (WT) and mutated (MUT) mouse *4ebp1* androgen response element (mARE) (right panel, 6 biological replicates, *P < 0.0001, ANOVA).

All scale bars = 100 μm. Data presented as mean +/− SEM.

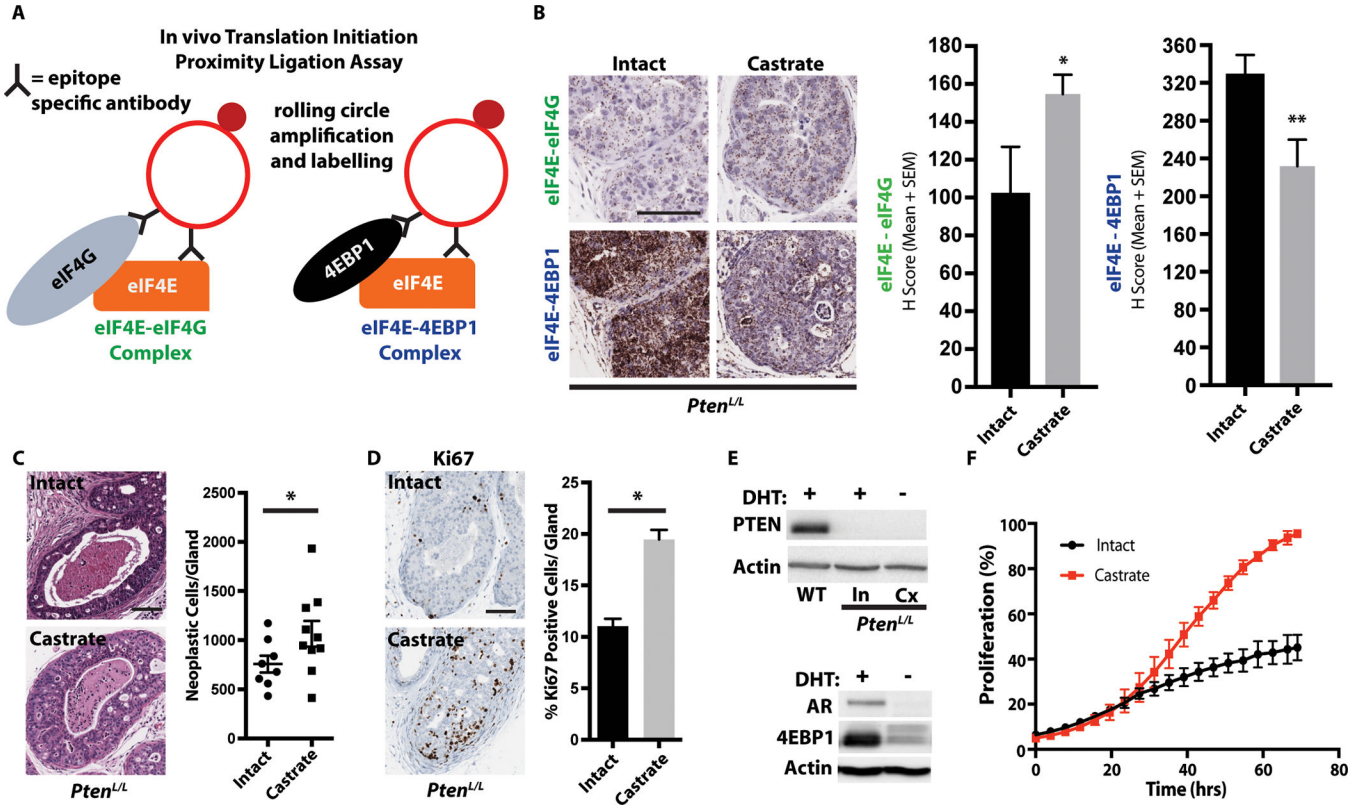

Figure 2. 4EBP1 expression controls eIF4E-eIF4G interaction dynamics and proliferation in a cell-autonomous manner.

(A) Schematic of the eIF4E-eIF4G and eIF4E-4EBP1 proximity ligation assays, which allow for the quantification of eIF4F translation initiation complexes and 4EBP1 inhibitory complexes in vivo.

(B) Representative images of the eIF4E-eIF4G and eIF4E-4EBP1 proximity ligation assays in intact and 8-week castrate *Pten*$^{L/L}$ ventral prostates (left panel). Quantification of the proximity ligation assay (right panel, intact n = 6, castrate n = 7, *P = 0.03, **P = 0.009, t-test).

(C) Representative hematoxylin and eosin staining of intact and 8-week castrate *Pten*$^{L/L}$ ventral prostates (left panel), with quantification (right panel, intact n = 8, castrate n = 10, *P = 0.04, t-test).

(D) Representative Ki67 staining of intact and 8-week castrate *Pten*$^{L/L}$ ventral prostates (left panel), with quantification [right panel, intact n = 7 (151 glands quantified), castrate n = 9 (206 glands quantified), *P < 0.0001, t-test].

(E) Representative western blot for PTEN and actin in wild-type (WT), intact *Pten*$^{L/L}$, and 8-week castrate *Pten*$^{L/L}$ primary organoids (top panel). Representative western blot for AR, 4EBP1, and actin in intact *Pten*$^{L/L}$ and 8-week castrate *Pten*$^{L/L}$ primary organoids (bottom panel).

(F) Growth curves of intact and castrate *Pten*$^{L/L}$ primary cells (3 biological replicate, P = 0.03, t-test).

All scale bars = 100 μm. Data presented as mean +/− SEM.

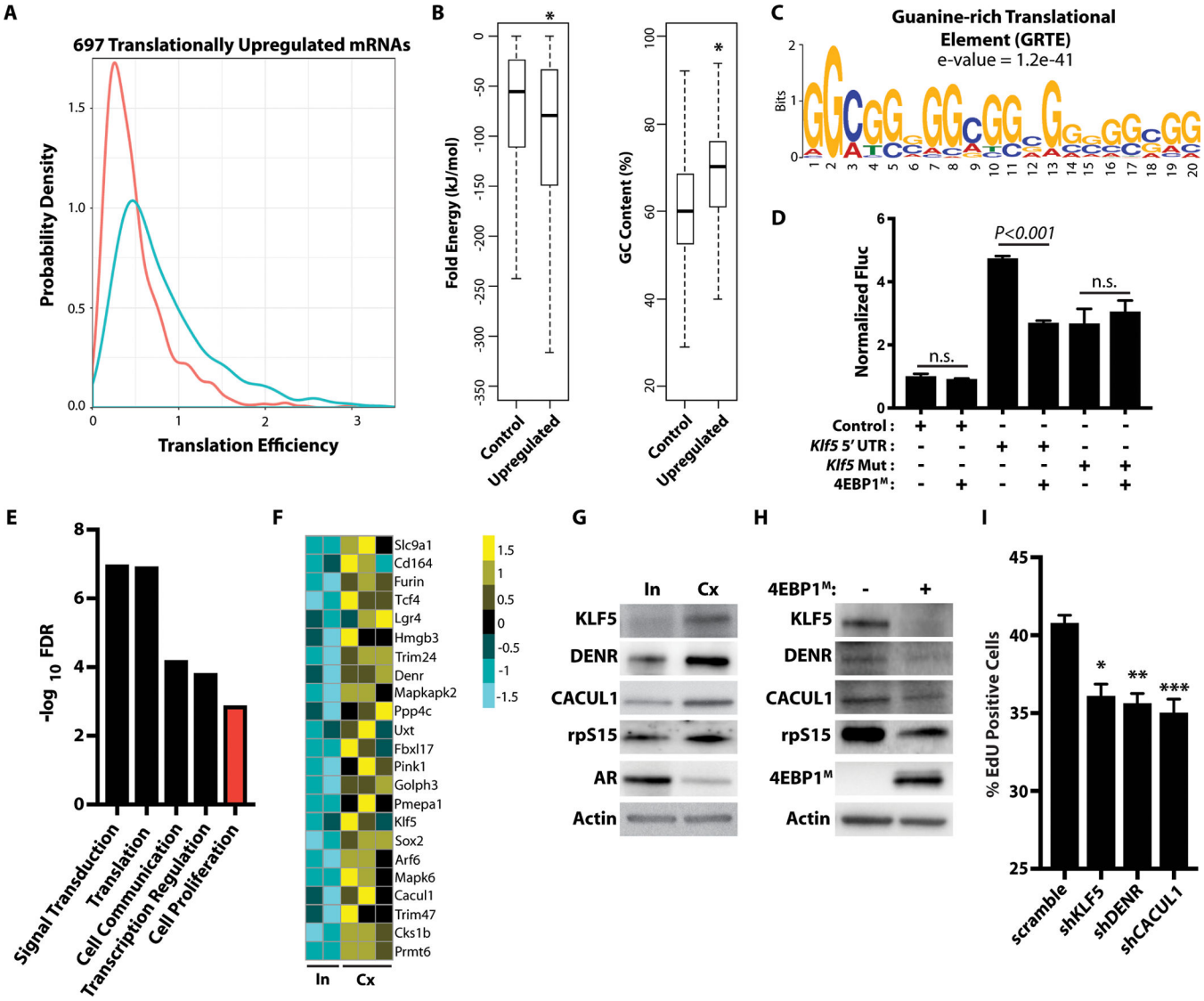

Figure 3. AR and eIF4F-mediated mRNA-specific translation controls a regulon of functional cell proliferation regulators

(A) Probability density graph of 697 translationally upregulated mRNAs between intact (n = 2) and castrate (n = 3) *Pten*$^{L/L}$ ventral prostates. Translation efficiency = ribosome-bound mRNA/total mRNA (P < 2.2e-16, Kolmogorov-Smirnov Test).

(B) Folding energy (P = 0.004339) and %GC content (P < 2.2e-16) between 5' UTRs of control mRNA (n = 19009) and upregulated mRNA (n = 187, t-test). Whiskers represent 1.5 times the interquartile range.

(C) The GRTE consensus sequence (e-value = 1.2e-41).

(D) Luciferase assay of the control vector, wild-type *Klf5* 5' UTR luciferase construct, and its GRTE deletion mutant with or without 4EBP1^{M} induction. Luciferase assay was normalized to *luc* and *RPS19* mRNA (n.s. = not statistically significant, n > 3 biological replicates/condition, t-test). Data presented as mean +/− SEM.

(E) Gene set enrichment analysis of the translationally up-regulated mRNA (log_2 fold change ≥ 0.75, FDR < 0.1) in castrate *Pten*$^{L/L}$ mice.

(F) Heatmap of translationally upregulated proliferation regulators in AR-low prostate cancer (log_2 fold change ≥ 0.75, FDR < 0.1).

(G) Representative western blot analysis of KLF5, DENR, CACUL1, rpS15, AR, and actin in primary intact (In = intact, DHT +) and castrate (Cx = castrate, DHT-) *Pten*$^{L/L}$ organoids.

(H) Representative western blot analysis of KLF5, DENR, CACUL1, rpS15, AR, and actin in primary *Pten*$^{L/L}$;*4ebp1*^{M} organoids with or without 4EBP1^{M} induction.

(I) Cell proliferation EdU incorporation assay in scramble, shKLF5, shDENR, or shCACUL castrate (DHT-) *Pten*$^{L/L}$ primary cells (replicate of 4–6 per condition, *P = 0.02, **P < 0.0001, ***P = 0.0003, t-test). Data presented as mean +/− SEM.

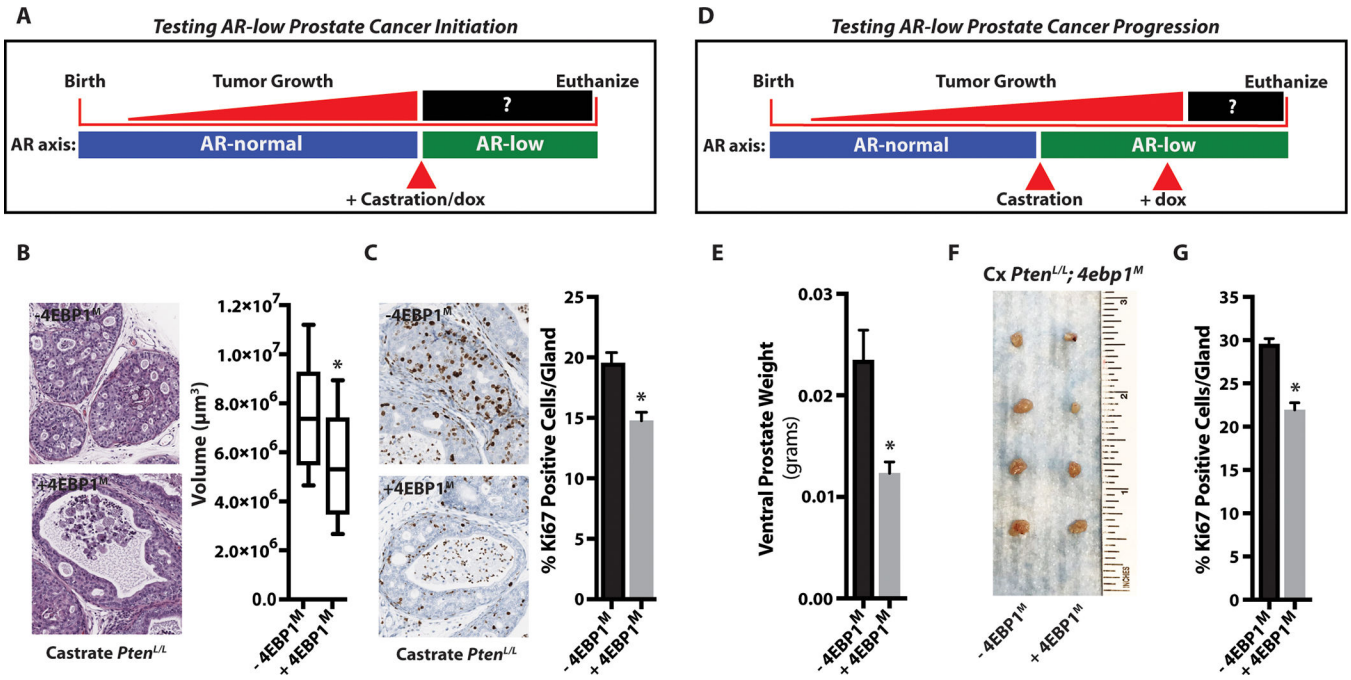

Figure 4. Increased eIF4F complex formation is necessary for AR-low prostate cancer initiation and progression.

(A) Schematic diagram of testing the impact of inhibiting eIF4F complex formation on AR-low prostate cancer initiation. *Pten*$^{L/L}$*;4ebp1*^{M} mice were castrated and immediately put on vehicle or doxycycline (dox) for 8 weeks.

(B) Representative hematoxylin and eosin staining of vehicle-treated (−4EBP1^{M}) and doxycycline-treated (+4EBP1^{M}) *Pten*$^{L/L}$*;4ebp1*^{M} ventral prostates (left panel). Quantification of tumor volumes after 8 weeks of inhibition of eIF4F complex formation started immediately after castration (right panel, vehicle - n = 9, doxycycline - n = 9, *P = 0.04).

(C) Representative Ki67 staining of vehicle-treated (−4EBP1^{M}) and doxycycline-treated (+4EBP1^{M}) *Pten*$^{L/L}$*;4ebp1*^{M} ventral prostates (left panel). Ki67 quantification after 8-week castration and immediate vehicle or doxycycline treatment [right panel, vehicle - n = 9 (205 glands quantified), doxycycline - n = 8 (169 glands quantified), *P < 0.0001, t-test].

(D) Schematic diagram of testing the impact of inhibiting eIF4F assembly on AR-low prostate cancer progression. *Pten*$^{L/L}$*;4ebp1*^{M} mice were castrated and allowed to form AR-low tumors for 12 weeks followed by an additional 12-week vehicle or doxycycline (dox) treatment.

(E) *Pten*$^{L/L}$*;4ebp1*^{M} ventral prostate weights after 12-week castration followed by an additional 12-week vehicle or doxycycline treatment (vehicle - n = 10, doxycycline - n = 9, *P = 0.0018, t-test).

(F) Representative images of *Pten*$^{L/L}$*;4ebp1*^{M} ventral prostates with or without *4ebp1*^{M} induction in the progression experiment.

(G) *Pten*$^{L/L}$*;4ebp1*^{M} ventral prostate Ki67 quantification after 12-week castration followed by an additional 12-week vehicle or doxycycline treatment [vehicle - n = 9 (197 glands quantified), doxycycline - n = 7 (139 glands quantified), *P < 0.0001, t-test].

All scale bars = 100 μm. Data presented as mean +/− SEM.

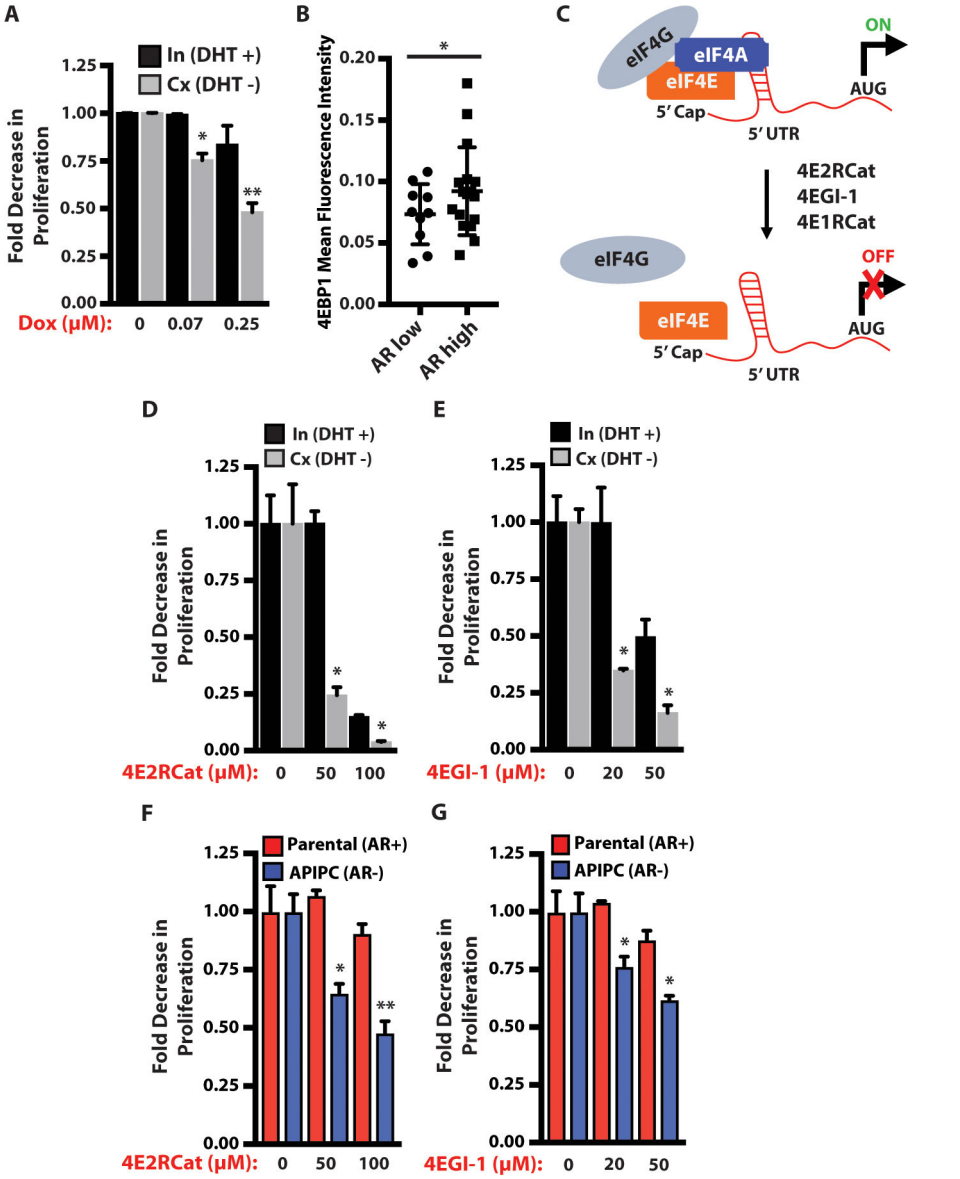

Figure 5. AR-low prostate cancer is more sensitive to disruption of the eIF4E-eIF4G interaction than AR-intact prostate cancer.

(A) Intact and castrate *Pten*$^{L/L}$;*4ebp1*^{M} primary prostate cancer cells treated with doxycycline for 48 hours. Proliferation was measured using the IncuCyte platform (In = intact, Cx = castrate, assay completed in triplicate, *P = 0.0026, **P = 0.03, t-test).

(B) 4EBP1 protein immunofluorescence quantification of a tissue microarray composed of end-stage metastatic CRPC patient specimens classified by AR protein expression (2–4 tumors sampled per patient, AR low - n = 10, AR high - n = 17, *P = 0.0089, t-test).

(C) Simplified schematic of the mechanism of action of 4E1RCat, 4E2RCat, and 4EGI-1, which disrupt the eIF4E-eIF4G interaction.

(D) Intact and castrate *Pten*$^{L/L}$ cells treated with 4E2RCat for 48 hours. Proliferation was measured using the IncuCyte platform (In = intact, Cx = castrate, assay completed in triplicate, *P < 0.0001, t-test).

(E) Intact and castrate *Pten*$^{L/L}$ cells treated with 4EGI-1 for 48 hours. Proliferation was measured using the IncuCyte platform (In = intact, Cx = castrate, assay completed in triplicate, *P = 0.002, t-test).
(F) AR+ parental and AR- APIPC prostate cancer cells treated with 4E2RCat for 48 hours. Proliferation was measured using the IncuCyte platform (assay completed in triplicate, *P < 0.0001, **P = 0.0003, t-test).
(G) AR+ parental and AR- APIPC prostate cancer cells treated with 4EGI-1 for 48 hours. Proliferation was measured using the IncuCyte platform (assay completed in triplicate, *P = 0.0003, t-test).
Data presented as mean +/− SEM.

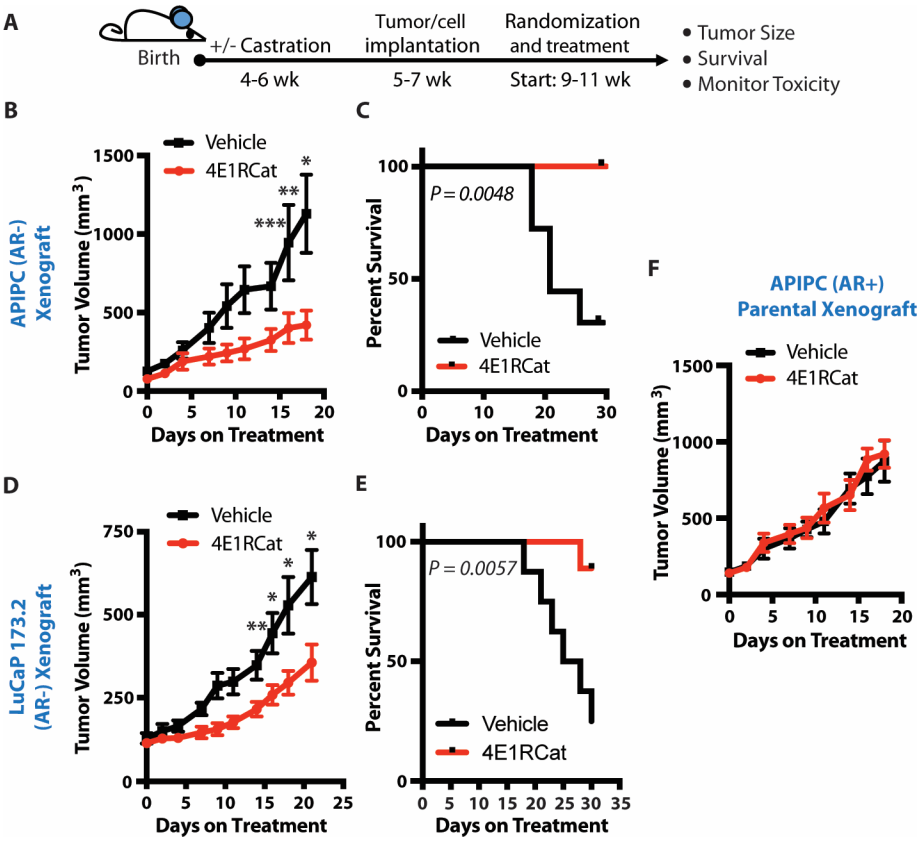

Figure 6. Targeting the eIF4E-eIF4G interaction in AR-deficient prostate cancer decreases tumor growth and improves survival.

(A) Schematic of the eIF4E-eIF4G interaction inhibitor preclinical trials.

(B) AR- APIPC xenograft preclinical trial testing the efficacy of 4E1RCat on AR-low prostate cancer tumor growth. Castrated mice were treated with 15 mg/kg 4E1RCat or vehicle (n = 8 – 4E1RCat-treated, n = 7 - vehicle-treated mice, *P = 0.0124, **P = 0.045, ***P = 0.05, t-test).

(C) AR- APIPC xenograft preclinical trial testing the impact of 4E1RCat on AR-low prostate cancer survival. Castrated mice were treated with 15 mg/kg 4E1RCat or vehicle (n = 8 – 4E1RCat-treated, n = 7 - vehicle-treated mice, P = 0.0048, log-rank test).

(D) LuCaP 173.2 PDX preclinical trial testing the efficacy of 4E1RCat on AR-low prostate tumor growth. Castrated mice were treated with 15 mg/kg 4E1RCat or vehicle (n = 9 – 4E1RCat-treated, n = 8 - vehicle-treated mice, *P = 0.02, **P = 0.01, t-test).

(E) LuCaP 173.2 PDX preclinical trial testing the impact of 4E1RCat in AR-low prostate cancer survival. Castrated mice were treated with 15 mg/kg 4E1RCat or vehicle (n = 9 – 4E1RCat-treated, n = 8 - vehicle-treated mice, P = 0.0057, log-rank test).

(F) AR+ parental APIPC xenograft preclinical trial testing the efficacy of 4E1RCat on AR+ prostate cancer tumor growth. Uncastrated mice were treated with 15 mg/kg 4E1RCat or vehicle (n = 8 – 4E1RCat-treated, n = 7 - vehicle-treated mice).

Data presented as mean +/− SEM.